Principal Component Analysis of Wind Profiler Observations

CHRISTOPHER R. WILLIAMS

Cooperative Institute for Research in the Environmental Sciences, University of Colorado and National Oceanic and Atmospheric Administration, Aeronomy Laboratory, Boulder, Colorado

(Manuscript received 8 March 1996, in final form 11 October 1996)

ABSTRACT

Principal component analysis (PCA) is applied to wind profiler observations to study the vertical profile of the wind field and its temporal evolution. The rationale for decomposing time–height wind profiler data using PCA is twofold. The orthogonal vertical profile vectors are determined empirically from the variance of the observations, and the time evolutions of these vectors are not simple sinusoids, but are temporal varying signals that can be directly related to other measurements. As an example of its utility, PCA is used to compare the annual and interannual variation of zonal wind measured with a 50-MHz VHF wind profiler above Christmas Island, Kiribati, with the difference between surface pressures measured at Tahiti, French Polynesia, and Darwin, Australia. The high correlation coefficients relate the vertical profile of zonal wind observed in the central Pacific with the variation of convection in the western Pacific. Complex PCA (C-PCA) allows the analysis of data consisting of amplitude and phase information. It can describe the phase progression of oscillations embedded within the data. The C-PCA is applied to VHF wind profiler observations to study the seasonal behavior of the diurnal meridional wind observed above Biak, Indonesia, and the oscillatory structures of the vertical wind during a convective precipitation event observed above Darwin.

1. Introduction

Modern analysis of atmospheric and oceanic data requires a variety of techniques. Principal component analysis (PCA) is used to decompose data into patterns and to reveal the time evolution of these patterns. The patterns, eigenvectors determined empirically from the data, are called empirical orthogonal functions (EOFs). The eigenvalues represent the amount of variance described by each eigenvector. Projection of the EOF onto the original data determines the EOF's time evolution and is called the principal component (PC).

Principal component analysis is a well-defined analysis technique used in contemporary studies by many sciences including archeology, medicine, and sociology. The most common use of PCA in meteorological data is the time evolution of standing oscillations in latitude versus longitude data at a single model level or altitude (Legler 1983; Hansen and Sutera 1992; Chang and Mak 1993; Kayano et al. 1995). The EOFs span the two-dimensional latitude versus longitude domain, and the PCs describe the EOF time evolution. PCA has been applied to individual station data or to ensembles of station data to study the vertical structure of observations above those stations (Blackmon et al. 1979; Gutzler and Harrison 1987; Gutzler 1990; Alexander et al. 1993; Fraedrich et al. 1993; Basu et al. 1995). PCA can be extended to complex data (yielding complex PCA, or C-PCA) to study propagating oscillations in the data (Barnett 1983; Horel 1984; Gutzler and Harrison 1987; Preisendorfer 1988).

The NOAA Aeronomy Laboratory has deployed VHF and UHF wind profilers across the tropical Pacific to measure winds and precipitation throughout the troposphere (Gage et al. 1990, 1991; Carter et al. 1995). These profilers provide high-temporal and high-vertical-resolution measurements that are well suited for dynamical studies of the atmosphere. PCA and C-PCA can be used in conjunction with other analysis techniques (e.g., Fourier analysis) to describe the observations and relate these observations with other measurements and to theories.

This paper presents four different examples of PCA applied to wind profiler observations. Section 2 of this paper briefly introduces PCA and the wind profiler data used in subsequent sections. The annual and interannual variation of zonal wind observed above Christmas Island, Kiribati, analyzed using PCA, is presented in section 3. Sections 4 and 5 discuss C-PCA applied to oscillating wind motions over Biak, Indonesia, and Darwin, Australia. Section 6 summarizes the utility of PCA applied to wind profiler observations.

2. PCA and wind profiler observations

The ultimate purpose of PCA, as presented in this paper, is to represent two-dimensional time–height wind

Corresponding author address: Dr. Christopher R. Williams, CIRES/NOAA/Aeronomy Laboratory, R/E/AL3, 325 Broadway, Boulder, CO 80303-3328.
E-mail: chris@a1.noaa.gov

profiler observations, with eigenvectors describing the wind vertical structure, and principal components describing the time evolution of these vectors. PCA and C-PCA are well-established techniques and the reader is referred to North et al. (1982), Barnett (1983), Horel (1984), North (1984), Richman (1986), or Preisendorfer (1988) for more details. The purpose of the following subsections is to introduce the structure of PCA and the wind profiler observations used in this study.

a. Outline of PCA and C-PCA

Let $D(t, z)$ be a set of time–height wind anomalies that are either scalar and real (e.g., zonal wind), or vectorial and expressed with real and imaginary components (e.g., diurnal wind oscillation). For simplicity, let $t = (1, \ldots, n)$ and $z = (1, \ldots, m)$. The covariance matrix of dimension $m \times m$ is computed using

$$S(z_1, z_2) = \mathbf{S} = \frac{1}{n-1} \sum_{t=1}^{n} D(t, z_1) D(t, z_2)^*, \quad (1)$$

where the asterisk indicates complex conjugation. If the wind anomalies are scalar values, the complex conjugation is superfluous. The eigenstructures of the covariance matrix are determined by solving the eigenproblem

$$\mathbf{SE} = \mathbf{E\Lambda}, \quad (2)$$

where the eigenvectors and eigenvalues are

$$\mathbf{E} = E(z, m) \equiv [e_1(z), \ldots, e_m(z)] \quad (3)$$

$$\mathbf{\Lambda} = \Lambda(m, m) \equiv \text{diag}(\lambda_1, \ldots, \lambda_m). \quad (4)$$

The principal components $\mathbf{A}$ of the eigenvectors are determined by projecting the eigenvectors onto the original wind anomalies. The original wind anomalies are reconstructed using

$$\mathbf{D} = (\mathbf{DE}^*)\,\mathbf{E}^{\mathrm{T}} = \mathbf{AE}^{\mathrm{T}}, \quad (5)$$

or expressed in scalar notation as

$$D(t, z) = \sum_{j=1}^{m} a_j(t)\, e_j(z). \quad (6)$$

The original wind anomalies are expressed in (6) as a linear combination of eigenvectors multiplied by their time evolution. A truncated set of EOFs can be used as a filter to extract or distinguish signals from noise. This filter is expressed as

$$D(t, z) = \sum_{j=1}^{p} a_j(t)\, e_j(z) + \sum_{j=p+1}^{m} a_j(t)\, e_j(z). \quad (7)$$

The summation of modes $j = (1, \ldots, p)$ represents the signal. Similarly, the summation of modes $j = (p + 1, \ldots, m)$ represents the noise. The signal plus noise formulation of (7) can also be used to filter large variance noise from lower variance signal, if the noise structure is known a priori (Poon et al. 1993; Hickey et al. 1995).

b. Wind profiler observations

The NOAA Aeronomy Laboratory has deployed several 50-MHz (VHF) wind profilers across the equatorial Pacific basin to monitor the tropospheric winds (Gage et al. 1990, 1991). Data collected from three wind profilers are used in this study. The profilers have similar altitude resolution of approximately 2–18 km with 0.5-km resolution. The temporal resolution is approximately 6 min for two profilers and 90 s for the third profiler.

In section 3, the 6-min resolution zonal wind from nearly 10 years of observations at Christmas Island (2°N, 157°W) are reduced to monthly mean values to study the annual and interannual variability. Monthly mean values allow the direct comparison with the monthly surface pressure difference between Tahiti, and Darwin, which is used to determine Southern Oscillation index (SOI). In section 4, the 6-min meridional winds from over two years of observations at Biak (1°S, 136°E) are reduced to hourly values to aid in the analysis of seasonal diurnal wind oscillations. And in section 5, the 90-s data is used without averaging to study the vertical wind oscillations associated with a 20-h mesoscale convective event that passed directly over the profiler at Darwin (12°S, 131°E). These different temporal events were chosen to illustrate the utility of PCA applied to wind profiler observations.

3. Annual and interannual variability above Christmas Island

The VHF wind profiler at Christmas Island (2°N, 157°W) was installed in early 1986 and has provided wind observations on a nearly continuous basis (Gage et al. 1994). The zonal wind observed above Christmas Island from 1986 to early 1995 is shown in Fig. 1. The annual and interannual variability of the zonal wind can be seen in Fig. 1. The normalized monthly surface pressure difference between Tahiti and Darwin is the SOI and is used to indicate the strength of the Walker circulation and the phase of the El Niño cycle. PCA is used to relate the observed zonal winds with the SOI that associates the zonal wind with the diabatic heating from tropical convection.

a. Annual variability of zonal wind

A composite year was constructed to evaluate the annual variability of zonal wind observed above Christmas Island. This composite year was fabricated by averaging the monthly mean winds observed from April 1986 to April 1995. The composite year zonal wind displayed in Fig. 2 represents a two-dimensional matrix with 12 time elements and 35 altitude elements. The altitude elements are uniformly spaced approximately 0.5 km apart implying less mass is represented by Δz aloft than by Δz near the surface. Such uniform altitude

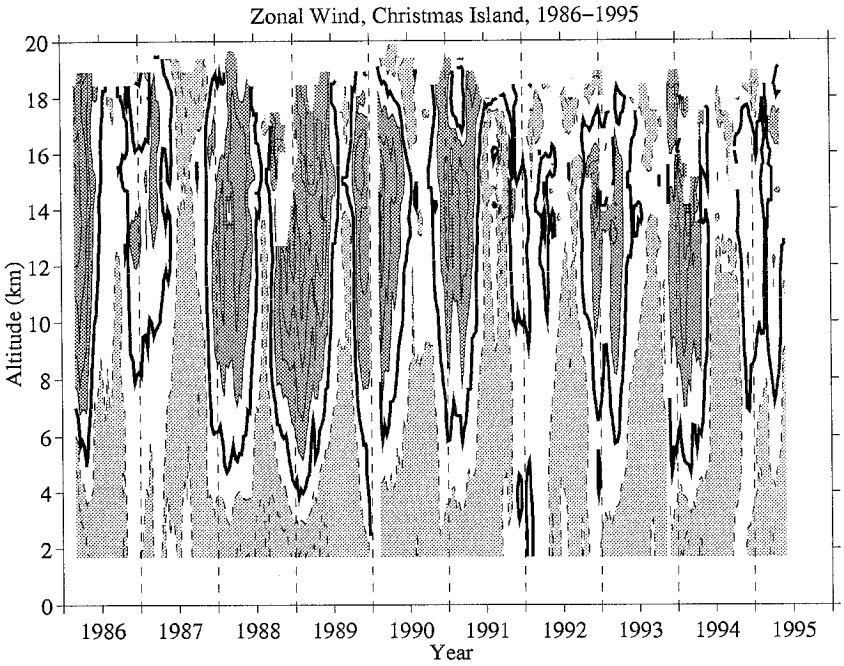

FIG. 1. Zonal wind measured above Christmas Island from April 1986 to April 1995. Dashed (solid) contours are easterlies (westerlies) at 5 m s^{-1} intervals; shading indicates magnitudes greater than 5 m s^{-1}.

spacing may be implicitly weighting higher altitude wind variances as compared to uniform pressure spacing as discussed in Blackmon et al. (1979) and Gutzler and Harrison (1987). The PCA was performed on this dataset yielding no more than 12 nonsingular eigenvectors and associated principal components. The percentages of contribution of the first three modes are listed in Table 1. Over 85% of the low-pass zonal wind variance can be explained by the first mode due to the simple baroclinic structure in this highly filtered data.

To illustrate the filtering features of PCA expressed in (7), Fig. 3 shows the reconstructed zonal wind using only the first two PCA modes ($p = 2$) plus the mean wind at each altitude. The eigenvectors have been normalized so that the relative contributions of each mode versus altitude can be compared directly between modes. The principal components have also been normalized so that the principal components each have root-mean-square (rms) values of unity. The reconstruction of the zonal wind can be verified by multiplying EOF_1 by PC_1 (by eye), and noticing the changes in sign at 9 km (where the annual mean wind is zero, not shown) near June and November. The time evolution of the eigenvector represented by the principal component is a fundamental concept of PCA.

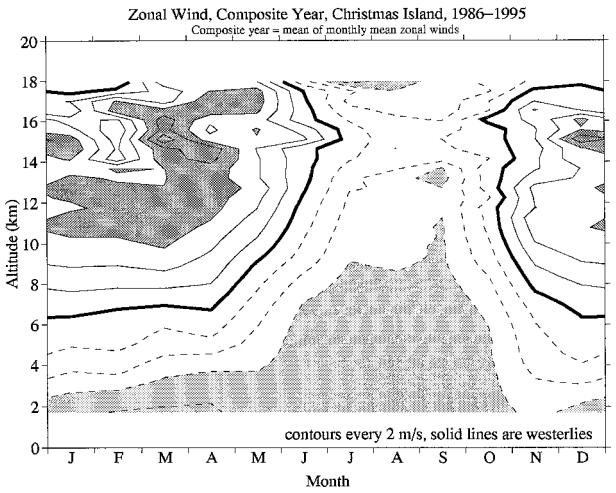

FIG. 2. Composite year of zonal wind above Christmas Island. The composite year is constructed by calculating the mean of the monthly mean winds. Dashed (solid) contours are easterlies (westerlies) at 2 m s^{-1} intervals; shading indicates magnitudes greater than 6 m s^{-1}.

TABLE 1. Principal component analysis.

Mode number	Eigenvalue*
Annual variation above Christmas Island (section 3a)	
1	85.2
2	6.3
3	3.8
Interannual variation above Christmas Island (section 3b)	
1	63.5
2	11.0
3	7.6

* All values are normalized to express percent variance.

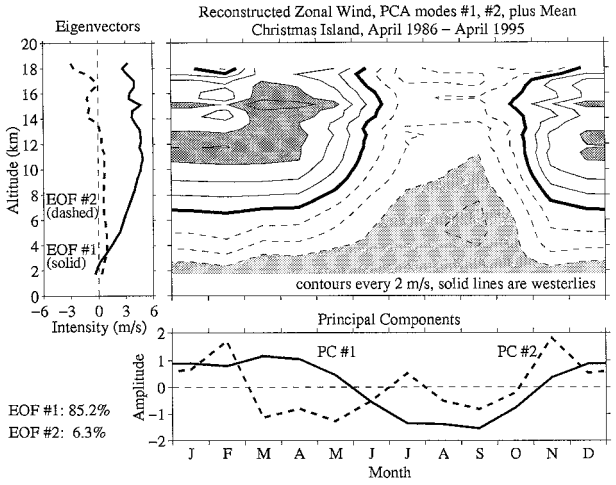

FIG. 3. Reconstructed zonal wind above Christmas Island using the first two PCA modes plus the mean wind at each altitude (center panel), EOFs for the first two PCA modes (left panel), and PCs for the first two PCA modes (bottom panel).

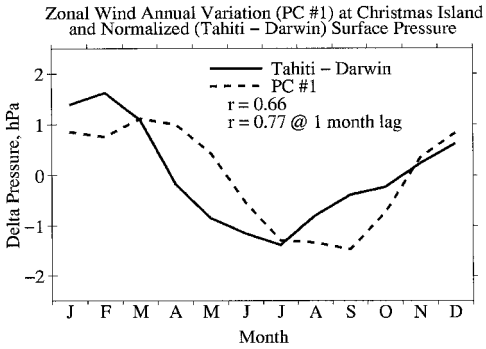

FIG. 4. Comparison of PC_1 (dashed) with the normalized (Tahiti minus Darwin) surface pressure (solid). The correlation coefficient is 0.67 at zero lag and 0.77 at 1-month lag.

The difference in surface pressure between Tahiti and Darwin is related to the tropical convection across the Pacific basin (Bjerknes 1969). Figure 4 compares the long-term mean annual variation in Tahiti-minus-Darwin surface pressure with PC_1. The correlation between the two curves is 0.67 at zero lag and 0.77 when the pressure difference curve lags by 1 month. The annual north–south movement of the centers of convection in the western Pacific lead to the temporal variation shown in Fig. 4. When the centers of convection are near the equator, upper-tropospheric westerly winds propagate to the east within the equatorial waveguide. These westerly winds are observed above Christmas Island in the central Pacific. The result of this comparison shows quantitative consistency between the annual variation of upper-tropospheric westerlies observed at Christmas Island and the annual variation in pressure difference between Tahiti and Darwin. See Gage et al. (1996a) for more details.

b. Interannual variation of zonal wind

The interannual variation of zonal wind observed above Christmas Island is investigated by removing the composite year winds from the monthly zonal wind. PCA was performed on the resulting monthly zonal wind anomalies and the percent contribution of the first three modes are presented in Table 1.

The first mode describes 63% of the zonal wind variability, with the normalized eigenvector and principal component shown in Fig. 5. The SOI is the standardized difference in surface pressure between Tahiti and Darwin and is plotted with PC_1 in Fig. 5. The SOI is a measure of the strength of the Walker circulation that results from the low-level convergence and upper-level divergence associated with convection distributed across the tropical Pacific basin (Bjerknes 1969; Webster 1972). The SOI is a good measure of the interannual variation of convection in the Pacific basin region. The correlation coefficient between SOI and PC_1 is 0.67.

During the El Niño of 1986–87 (negative SOI), tropical convection extended eastward from the western Pacific with increased surface precipitation recorded at Christmas Island (relative to the 10-yr record). The phase of the dominant mode reversed during the La Niña (positive SOI) of 1988–89, as convection was confined to the Indonesian Maritime Continent. The persistent El Niño condition from 1990 to 1994, as determined by the SOI and the zonal wind above Christmas Island, has been discussed by Trenberth and Hoar (1996) and Gage et al. (1996b). The correlation between SOI and PC_1 associates the strength and phase of the Walker circulation with an observed monthly mean zonal wind profile in the central Pacific.

4. Diurnal wind oscillations above Biak

A VHF profiler has been in near-continuous operation at Biak (1°S, 136°E) since early 1992. The hourly meridional winds are used to examine the seasonal variation of the diurnal wind that are assumed to result from the solar heating of water vapor and the latent heat release from diurnal varying convection. These forced

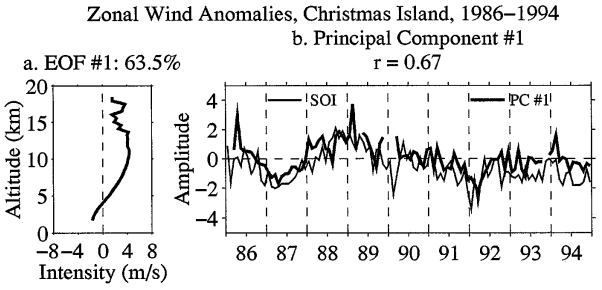

FIG. 5. EOF_1 for the interannual zonal wind above Christmas Island (left panel). Comparison of the interannual zonal wind PC_1 (thick line) with the SOI (thin line) (right panel).

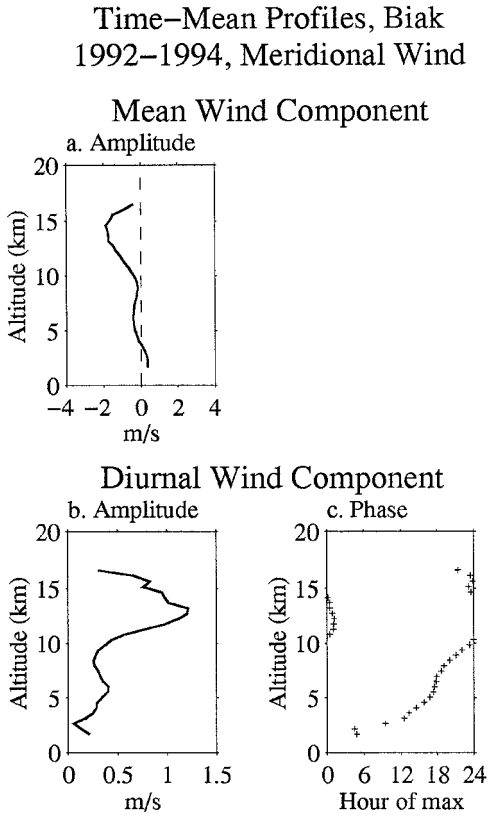

FIG. 6. Time-mean profiles of (a) meridional mean wind, (b) meridional diurnal wind amplitude, and (c) meridional diurnal wind phase observed above Biak. Phase is the hour of maximum southerly wind expressed in local solar time.

tropospheric oscillations may propagate upward into the stratosphere/mesosphere where they break and deposit horizontal momentum (Williams and Avery 1996a). In the troposphere, these seasonal diurnal winds have small amplitudes relative to the shifts in synoptic winds that can occur over a 24-h period. One way to extract these small-amplitude oscillations from the synoptic noise is to construct composite days using many days of observations (Williams and Avery 1996b). The composite day extracts coherent phase oscillations at each harmonic of 24 h.

To examine the change in seasonal meridional diurnal wind with time, composite days were constructed using a 91-day window that was shifted day-by-day through the data. For each composite day, the mean wind, diurnal, and semidiurnal wind oscillations were determined using a least squares fit analysis (Palo and Avery 1993). The mean wind is a scalar value and the diurnal wind is a vector expressed with real and imaginary components. Before PCA and C-PCA can be performed on these data, the time-mean values must be determined and are shown in Fig. 6. The vertical amplitude profiles of the meridional mean and diurnal wind are similar. They both have maximum amplitude near 14 km, a relative minimum near 9 km, and an increased amplitude

TABLE 2. Complex principal component analysis.

Mode number	Eigenvalue*
Meridional wind above Biak (section 4)	
1, mean wind	92.8
2, mean wind	3.1
3, mean wind	1.5
1, diurnal wind	58.8
2, diurnal wind	14.5
3, diurnal wind	8.8
Vertical velocity above Darwin (section 5)	
1	41.4
2	18.8
3	9.0

* All values are normalized to express percent variance.

near 5 km. The hour of maximum southerly diurnal wind increases with altitude from 2 to 12 km. The meridional wind phase structure is a result of downward propagation of energy and/or the observations are being made in the altitude range of active diurnal sources (Williams and Avery 1996b).

The percent contribution from the first three PCA and C-PCA modes are listed in Table 2. The first normalized EOF and PC for the mean and the diurnal meridional wind components are shown in Fig. 7. The diurnal meridional wind EOF and PC (Figs. 7c and 7d) are each represented with two curves. The solid line is the amplitude and the pluses are the hour of maximum southerly diurnal wind expressed in local solar time. The reconstruction of the diurnal wind amplitude consists of multiplying the EOF amplitude by the PC amplitude (with proper denormalization). The diurnal wind phase is reconstructed by *adding* the phases of the EOF and the PC. The absolute phase of the EOF is arbitrary with the phase of the dominant EOF at the lowest altitude set to zero by construction. All EOFs are orthogonal, and their phase is relative to the dominant mode. Both the EOF and PC must be examined to determine the phase at a particular time–height location of the reconstructed data.

The mean meridional wind EOF has a dominant upper-tropospheric structure and a smaller amplitude, out-of-phase component in the lower troposphere. The corresponding mean wind PC indicates an annual cycle with southerly (northerly) winds during the boreal winter (summer) above 10 km. Using satellite-derived highly reflective cloud indices, Waliser and Gautier (1993) charted the annual north–south movement of the centers of convection over the tropical Pacific and showed that during the boreal winter (summer) the convection is south (north) of Biak. The dominant meridional mean wind is consistent with the convection producing upper-tropospheric divergent winds observed at Biak.

The diurnal meridional wind EOF has its largest amplitude in the upper troposphere. The diurnal PC has an annual cycle that is in phase with the mean meridional wind PC. It has been shown that oceanic convection has

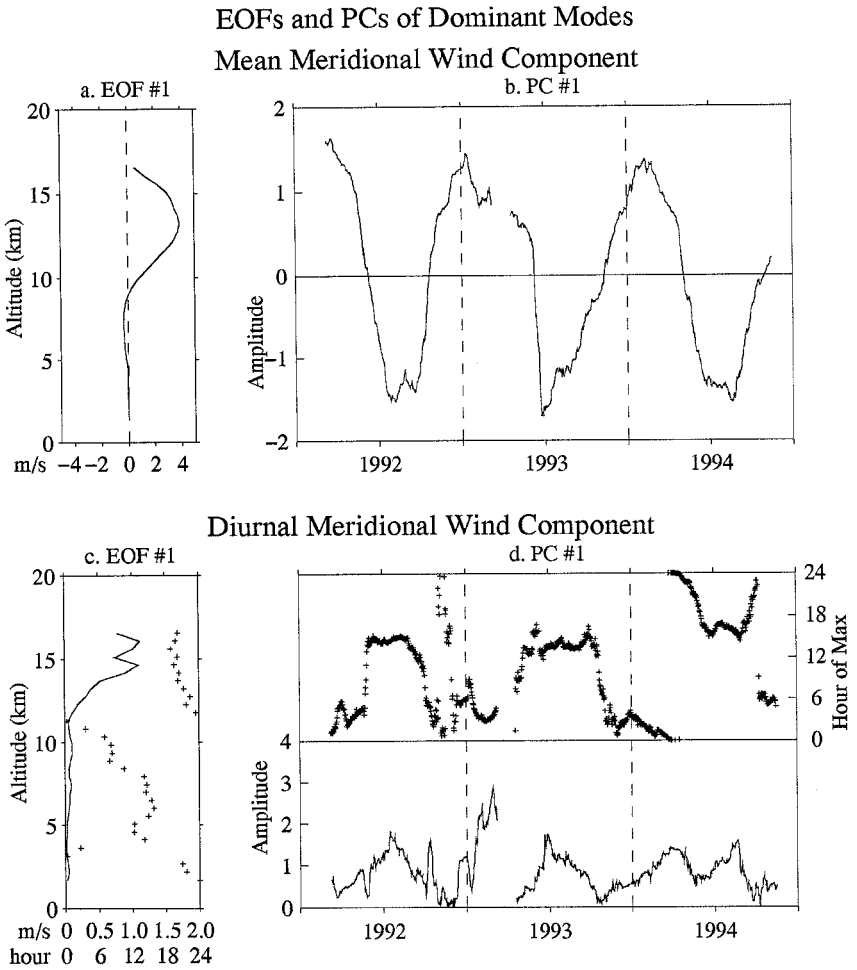

FIG. 7. EOFs and PCs for the dominant modes above Biak. (a) EOF_1 and (b) PC_1 for the meridional mean wind; (c) EOF_1 and (d) PC_1 for the meridional diurnal wind. Phase is the hour of maximum southerly wind expressed in local time.

a diurnal variation (Hendon and Woodberry 1993; Janowiak et al. 1994; Berg and Avery 1995; Williams and Avery 1996a). Assuming that the diurnal variation of convection has a diurnal varying diabatic heating rate, the coherency between the mean and diurnal wind PCs may be associated with the diurnal variability of convection.

5. Vertical wind motions during convective precipitation

One of the advantages of C-PCA over PCA is the ability to describe the oscillatory time evolution of the eigenvectors. This benefit is shown using vertical wind motions measured by the 50-MHz wind profiler located at Darwin (12°S, 131°E) when a convective precipitating cloud passed over the profiler. This precipitation event was monsoonal in structure containing convective cores imbedded in stratiform rain (Keenan and Rutledge 1993). Figure 8 shows the vertical winds measured by the profiler as well as the surface rain rate when this precipitating cloud system passed over the profiler. The convective and stratiform portions of this precipitation event were determined by analyzing the vertical velocities measured with a collocated 920-MHz UHF profiler and using the classification technique discussed in Williams et al. (1995). The increased rain rate and upward velocities in excess of 1 m s^{-1} shown in Fig. 8 indicate convective precipitation. The 50-MHz wind profiler can measure both the Bragg scattering from clear air and the Rayleigh scattering from the precipitation during strong rain events producing Doppler spectra with multiple peaks and convoluted peaks (May and Rajopadhyaya 1996). The first moment corresponding to the largest spectral peak was used as the measured vertical velocity estimate. Due to the possible selection of the precipitation Doppler velocity, the velocity estimate may have a negative bias (downward) relative to the actual air velocity. This limitation will affect the quantitative results but not the qualitative results of this work.

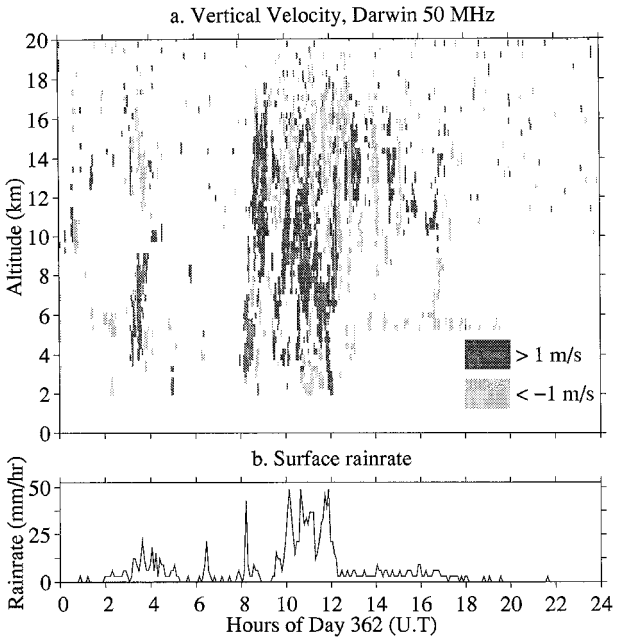

FIG. 8. (a) Vertical velocity measured with the 50-MHz wind profiler at Darwin. Dark (light) shading is upward (downward) motion with magnitudes greater than 1 m s^{-1}. (b) Rain rate determined from a surface rain gauge using a 5-min observation window.

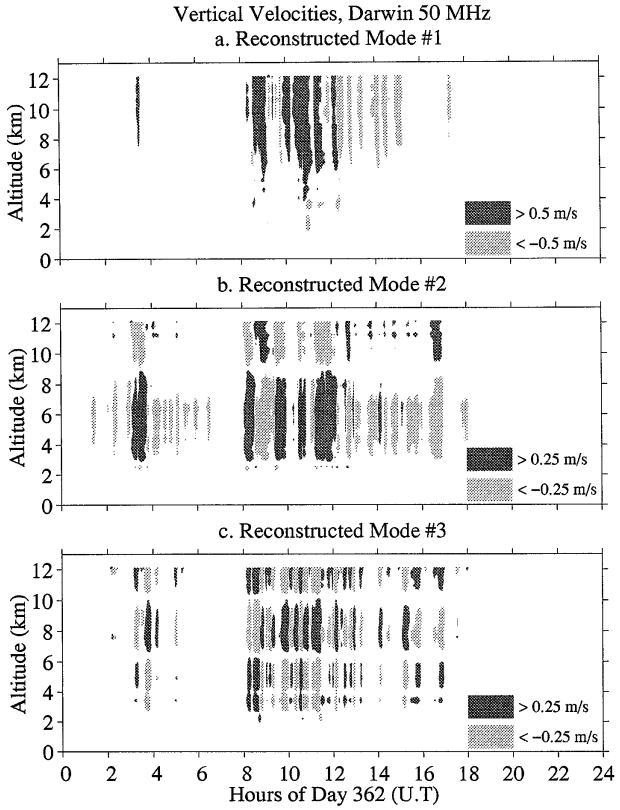

FIG. 9. Reconstructed vertical velocities above Darwin using individual C-PCA modes: (a) mode 1, (b) mode 2, and (c) mode 3. Dark (light) shading is upward (downward) motion.

The measured vertical velocities are scalar values and must be converted to vector values before performing the C-PCA. The real component of the vector is the observed wind. The imaginary component is the Hilbert transform of the observed wind. The Hilbert transform shifts the input data by $+90°$ ($\pi/2$ rad). The beginning and end of the vector time series need to be tapered to avoid erroneous C-PCA computations (Horel 1984). To ensure a near-full data matrix, the C-PCA was performed on the vertical wind velocities between the altitudes of 2–12 km. Table 2 lists the percent contribution by the first three modes of the C-PCA. The reconstructed vertical winds from the first three modes are shown in Fig. 9. Gamage and Blumen (1993) showed that decomposition of abrupt events using PCA and Fourier analysis may require many modes to represent the observations.

By construction, the three different modes shown in Fig. 9 capture different vertical structures. The dominant mode captures the strong upper-tropospheric updrafts associated with convective cores. The second mode has a bimodal structure with a phase change near 9 km. The third mode has two phase changes near 6 and 10 km. The EOFs and PCs for these three modes are shown in Fig. 10. The phase of each eigenvector is nearly constant with altitude except for abrupt phase changes occurring while the amplitude is near local minima. The profile of vertical wind captured by EOF_1 resembles the profiles of intense updrafts associated with convective cores with maximum updrafts above 8 km (Cifelli and Rutledge 1994; May and Rajopadhyaya 1996). The association of the dominant mode with deep convective rain is also indicated in the PC amplitudes shown in Fig. 10. During the convective rain and subsequent stratiform rain from 8 to 16 h, all three PCs have increased amplitude. In contrast, during the shallow rain event near hour 3, there is only a slight increase in PC_1 amplitude relative to the increased amplitudes in PC_2 and PC_3.

From Fig. 9, it can be seen that the time evolution of the three modes are different, with the third mode having more sinusoidal oscillations than the first mode. The instantaneous frequency of oscillation is calculated directly from the rate of change in PC phase and is shown in Fig. 10. The instantaneous frequency should be examined only when the PC amplitude is not near zero. The dominant mode is not a simple oscillating structure, but is arrhythmic with abrupt changes in intensity, phase, and frequency. The third mode has a more uniform oscillation frequency, yet varies between 0 and 4 cycles per hour. The second and third modes have vertical wavelengths of about 14 and 7 km and all three modes may represent gravity waves generated by the convective precipitation. Mapes and Houze (1995) postulate that gravity waves are generated by, and propagate away from, convective source regions. In addition, the propagation of convectively generated gravity waves from the troposphere upward and into the middle at-

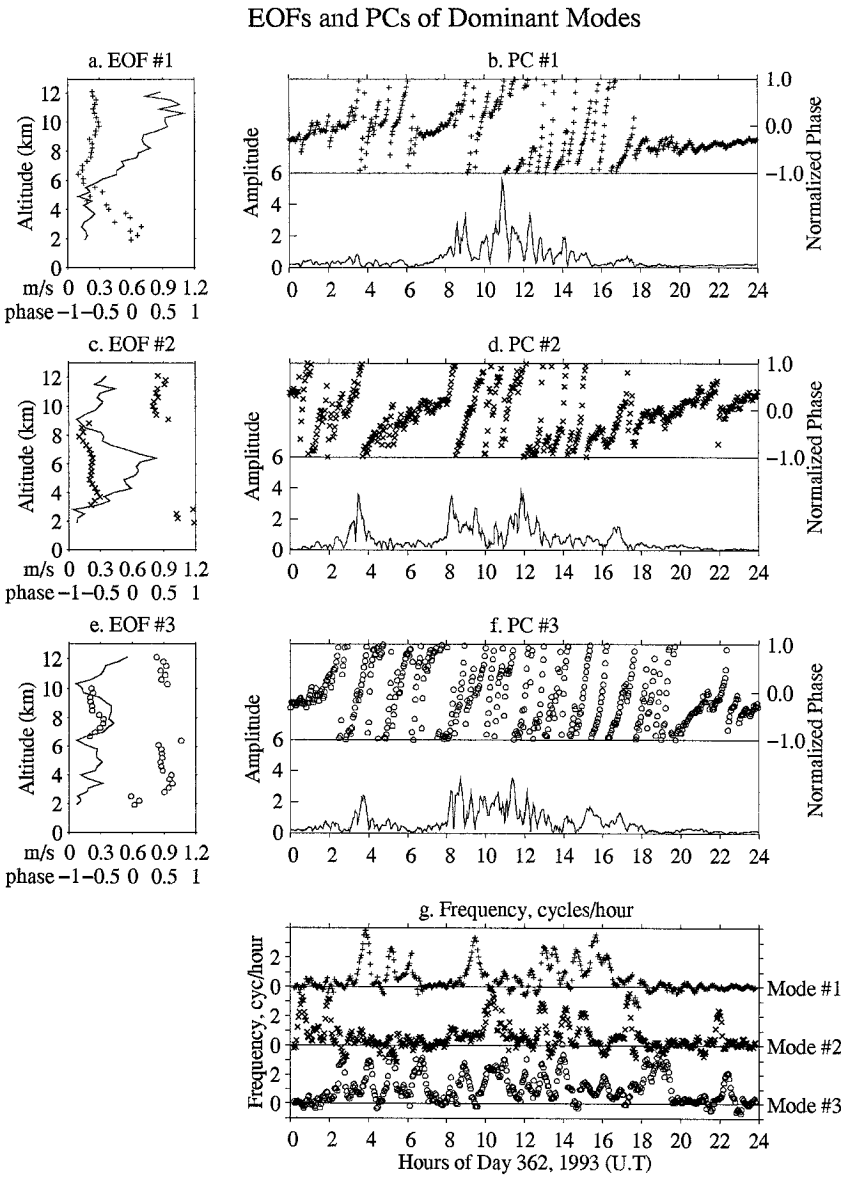

FIG. 10. EOFs and PCs for the first three vertical velocity C-PCA modes: (a) and (b) mode 1, (c) and (d) mode 2, and (e) and (f) mode 3. Normalized phase ranges from −1 to 1 and is equivalent to the radian phase range of $-\pi$ to π. (g) The instantaneous frequency of oscillation is the PC rate of change expressed in cycles per hour and has been filtered using a seven-point running mean.

mosphere has been modeled by Alexander (1996) using a linear ray tracing model. If the observed modes are gravity waves produced by convection, then their change in frequencies may represent the dispersion of energy, as these gravity waves propagate away from the convective source region and/or the change in frequency of the convective source as it matures and dissipates into stratiform rain. These interpretations cannot be refined without other datasets to determine the position and life cycle of the convective system observed passing over the profiler.

6. Conclusions

In this paper PCA and C-PCA were applied to wind profiler observations. These analysis techniques decomposed the time–height wind profiler observations into EOFs that describe the vertical profile and into PCs that describe the time evolution of these EOFs. PCA has benefits not available with other analysis techniques. PCA determines the fewest number of orthogonal functions that can describe the vertical structure embedded within the variance of the observations. The time evo-

lution of these vertical profiles are described with the PCs and are not simple sinusoids. They are time-varying signals that can be compared with other time series.

PCA is a mathematical analysis technique with limitations that need to be understood. PCA produces eigenvectors and eigenvalues from the observed data covariance matrix. The eigenvalues indicate the amount of variance described by each eigensolution. If two or more solutions describe the same amount of variance, within sampling errors, then the modes are degenerate. Solutions are degenerate if the original data have independent vertical structures each describing approximately the same amount of variance, or if the vertical structures embedded in the original data are nonstationary and change during the observation interval. Nonstationary vertical structures must be described using more than one EOF. Stationarity is also a constraint of Fourier analysis with a time domain oscillation that changes frequency being projected onto several spectral components.

PCA and C-PCA were applied to four different examples of wind profiler observations. In section 3, the annual and interannual variations of zonal wind above Christmas Island were analyzed using PCA. The dominant modes described over 85% and 63% of the annual and interannual variability. The PCs of these dominant modes were compared with the difference in surface pressure measured at Tahiti and Darwin. The high correlation coefficients related a vertical profile of zonal wind observed in the central Pacific to the deep tropical heating associated with convection in the western Pacific. The annual variation in zonal wind is related to the north–south movement of convection as described in Gage et al. (1996a) and the interannual variation is related to the east–west movement of convection associated with El Niño.

In section 4, C-PCA was applied to the diurnal meridional wind observed above Biak. The phase information provided by the C-PCA allowed the analysis of oscillating structures that is not possible with PCA. The phase of the dominant diurnal meridional wind mode above Biak was in phase with the north–south movement of the active centers of convection relative to Biak, suggesting a relation between diurnal oscillating convection and the observed diurnal wind.

The vertical wind measured above Darwin when a precipitating cloud passed over the profiler was studied in section 5. The observed scalar wind motions were converted to vectorial values using the Hilbert transform then decomposed into several C-PCA modes. The dominant mode represented the strong vertical updrafts associated with convective precipitation. The next two modes had shorter vertical wavelengths, and all three modes are believed to be part of the gravity waves spectra generated by the convective diabatic heating associated with the precipitation.

One of the benefits of C-PCA shown in this paper is the ability to track the phase progression of a particular mode. The change in PC phase indicates a phase shift in the EOF. The PC rate of change indicates instantaneous frequency. This interpretation can be applied to gravity wave propagation in a source-free region of the atmosphere with the positive (negative) phase progression indicating gravity wave energy propagation downward (upward) from the gravity wave source region.

Acknowledgments. The author thanks David Gutzler for helpful discussions of PCA and its application. The Christmas Island wind profiler was constructed and is being operated with the support of the U.S. TOGA Project Office. The NOAA/CU Trans Pacific Profiler Network is supported by the National Science Foundation under Agreements ATM-87220797 and ATM-9214800. A thank you is extended to Anthony Riddle for his contributions to the archival and quality control of the profiler data. The Biak profiler is operated in conjunction with the Indonesian National Institute of Aeronautics and Space, and the Darwin profiler is operated by the Australian Bureau of Meteorology Research Centre.

REFERENCES

Alexander, G. D., G. S. Young, and D. V. Ledvina, 1993: Principal component analysis of vertical profiles of Q_1 and Q_2 in the Tropics. *Mon. Wea. Rev.,* **121,** 535–548.

Alexander, M. J., 1996: A simulated spectrum of convectively generated gravity waves: Propagation from the tropopause to the mesopause and effects on the middle atmosphere. *J. Geophys. Res.,* **101,** 1571–1588.

Barnett, T. P., 1983: Interaction of the monsoon and Pacific trade wind system at interannual time scales. Part I: The equatorial band. *Mon. Wea. Rev.,* **111,** 756–773.

Basu, S., R. M. Gairola, C. M. Kishtawal, and P. C. Pandey, 1995: Empirical orthogonal function analysis of humidity profiles over the Indian Ocean and an assessment of their retrievability using satellite microwave radiometry. *J. Geophys. Res.,* **100,** 23 009–23 017.

Berg, W., and S. K. Avery, 1995: Evaluation of monthly rainfall estimates derived from the Special Sensor Microwave/Imager (SSM/I) over the tropical Pacific. *J. Geophys. Res.,* **100,** 1295–1316.

Bjerknes, J., 1969: Atmospheric teleconnections from the equatorial Pacific. *Mon. Wea. Rev.,* **97,** 163–172.

Blackmon, M. L., R. A. Madden, J. M. Wallace, and D. S. Gutzler, 1979: Geophysical variations in the vertical structure of geopotential height fluctuations. *J. Atmos. Sci.,* **36,** 2450–2466.

Carter, D. A., K. S. Gage, W. L. Ecklund, W. M. Angevine, P. E. Johnston, A. C. Riddle, J. Wilson, and C. R. Williams, 1995: Developments in lower tropospheric wind profiling at NOAA's Aeronomy Laboratory. *Radio Sci.,* **30,** 977–1001.

Chang, J. J.-C., and M. Mak, 1993: A dynamical empirical orthogonal function analysis of the intraseasonal disturbances. *J. Atmos. Sci.,* **50,** 613–630.

Cifelli, R., and S. A. Rutledge, 1994: Vertical motion structure in maritime continent mesoscale convective systems: Results from a 50-MHz profiler. *J. Atmos. Sci.,* **51,** 2631–2652.

Fraedrich, K., S. Pawson, and R. Wang, 1993: An EOF analysis of the vertical-time-delay structure of the quasi-biennial oscillation. *J. Atmos. Sci.,* **50,** 3357–3365.

Gage, K. S., B. B. Balsley, W. L. Ecklund, R. F. Woodman, and S. K. Avery, 1990: Wind-profiling Doppler radars for tropical atmospheric research. *Eos,* **71,** 1851–1854.

——, ——, ——, D. A. Carter, and J. R. McAfee, 1991: Wind profiler

related research in the tropical Pacific. *J. Geophys. Res.,* **96,** 3209–3220.

——, J. R. McAfee, W. L. Ecklund, D. A. Carter, C. R. Williams, P. E. Johnston, and A. C. Riddle, 1994: The Christmas Island wind profiler: A prototype VHF wind-profiling radar for the Tropics. *J. Atmos. Oceanic Technol.,* **11,** 22–31.

——, ——, and C. R. Williams, 1996a: On the annual variation of tropospheric zonal winds observed above Christmas Island in the central equatorial Pacific. *J. Geophys. Res.,* **101,** 15 061–15 070.

——, ——, and ——, 1996b: Recent changes in tropospheric circulation over the central equatorial Pacific. *Geophys. Res. Lett.,* **23,** 2149–2152.

Gamage, N., and W. Blumen, 1993: Comparative analysis of low-level cold fronts: Wavelet, Fourier, and empirical orthogonal function decompositions. *Mon. Wea. Rev.,* **121,** 2867–2878.

Gutzler, D. S., 1990: Vertical structure and interannual variability of tropical zonal winds. *J. Climate,* **3,** 741–750.

——, and D. E. Harrison, 1987: The structure and evolution of seasonal wind anomalies over the near-equatorial eastern and western Pacific Oceans. *Mon. Wea. Rev.,* **115,** 169–192.

Hansen, A. R., and A. Sutera, 1992: Structure in the phase space of a general circulation model deduced from empirical orthogonal functions. *J. Atmos. Sci.,* **49,** 320–326.

Hendon, H. H., and K. Woodberry, 1993: The diurnal cycle of tropical convection. *J. Geophys. Res.,* **98,** 16 623–16 637.

Hickey, K., R. H. Khan, and J. Walsh, 1995: Parametric estimation of ocean surface currents with HF radar. *IEEE J. Oceanic Eng.,* **20,** 139–144.

Horel, J. D., 1984: Complex principal component analysis: Theory and examples. *J. Climate Appl. Meteor.,* **23,** 1660–1672.

Janowiak, J. E., P. A. Arkin, and M. Morrissey, 1994: An examination of the diurnal cycle in oceanic tropical rainfall using satellite and in situ data. *Mon. Wea. Rev.,* **122,** 2296–2311.

Kayano, M. T., V. E. Kousky, and J. E. Janowiak, 1995: Outgoing longwave radiation bias and their impacts on EOF modes of interannual variability in the Tropics. *J. Geophys. Res.,* **100,** 3173–3195.

Keenan, T. D., and S. A. Rutledge, 1993: Mesoscale characteristics of monsoonal convection and associated stratiform precipitation. *Mon. Wea. Rev.,* **121,** 352–374.

Legler, D. M., 1983: Empirical orthogonal function analysis of wind vectors over the tropical Pacific region. *Bull. Amer. Meteor. Soc.,* **64,** 234–241.

Mapes, B. E., and R. A. Houze Jr., 1995: Diabatic divergence profiles in western Pacific mesoscale convective systems. *J. Atmos. Sci.,* **52,** 1807–1828.

May, P. T., and D. K. Rajopadhyaya, 1996: Wind profiler observations of vertical motion and precipitation microphysics of a tropical squall line. *Mon. Wea. Rev.,* **124,** 807–815.

North, G. R., 1984: Empirical orthogonal functions and normal modes. *J. Atmos. Sci.,* **41,** 879–886.

——, T. L. Bell, R. F. Cahalan, and F. J. Moeng, 1982: Sampling errors in the estimation of empirical orthogonal functions. *Mon. Wea. Rev.,* **110,** 699–706.

Palo, S. E., and S. K. Avery, 1993: Mean winds and the semiannual oscillation in the mesosphere and lower thermosphere at Christmas Island. *J. Geophys. Res.,* **98,** 20 385–20 400.

Poon, M. W. Y., R. H. Khan, and S. Le-Ngoc, 1993: A singular value decomposition (SVD) based method for suppressing ocean clutter in high frequency radar. *IEEE Trans. Signal Processing,* **41,** 1421–1425.

Preisendorfer, R. W., 1988: *Principal Component Analysis in Meteorology and Oceanography.* Elsevier Science, 425 pp.

Richman, M., 1986: Rotation of principal components. *J. Climatol.,* **6,** 293–335.

Trenberth, K. E., and T. J Hoar, 1996: The 1990–95 El Niño–Southern Oscillation event: Longest on record. *Geophys. Res. Lett.,* **23,** 57–60.

Waliser, D. E., and C. Gautier, 1993: A satellite-derived climatology of the ITCZ. *J. Climate,* **6,** 2162–2174.

Webster, P. J., 1972: Response of the tropical atmosphere to local steady forcing. *Mon. Wea. Rev.,* **100,** 518–540.

Williams, C. R., and S. K. Avery, 1996a: Diurnal nonmigrating tidal oscillations forced by deep convective clouds. *J. Geophys. Res.,* **101,** 4079–4091.

——, and ——, 1996b: Diurnal winds observed in the tropical troposphere using 50 MHz wind profilers. *J. Geophys. Res.,* **101,** 15 051–15 060.

——, W. L. Ecklund, and K. S. Gage, 1995: Classification of precipitating clouds in the Tropics using 915-MHz wind profilers. *J. Atmos. Oceanic Technol.,* **12,** 996–1012.